2005 American Control Conference
June 8-10, 2005. Portland, OR, USA

Design and DSP Microprocessor Implementation of Digital Sinusoidal Tracking Controllers **

B. C. Chang*
bchang@coe.drexel.edu

Chunlong Hu
chu@drexel.edu

Mark Ilg
emerican@drexel.edu

Department of Mechanical Engineering and Mechanics
Drexel University, Philadelphia, PA 19104

***Abstract* – The flight control of a spinning flying vehicle may be more involved than that of a missile or even an aircraft since the actuators are on a rotating frame instead of a fixed one. One possible solution is to oscillate the canards according to the spinning frequency and phase of the vehicle so that the deflection of the canards seen from the earth is unaffected by the spinning. The problem becomes a sinusoidal tracking control problem that can be solved by the discrete-time optimal regulator/tracking control theory. Both the frequency and time domain aspects of the design are discussed. The designed tracking controller will be implemented on a DSP microprocessor. Some practical issues arising in the implementation will be also addressed.**

Keywords – Flight control of spinning vehicles, Optimal regulator/tracking control theory, Discrete-time control, DSP microprocessor control.

I. INTRODUCTION

The sinusoidal tracking control problem considered in the paper arises in the control of spinning flying vehicles like rockets or flying munitions systems. It has been a common practice to incorporate a persistent spin to a cylindric flying vehicle to stabilize its heading direction. However, the spin would cause a challenge in controller design if the flight path needs to be altered during the flight. Unlike the flight control of missiles or aircrafts, which have no persistent spin, the flight path actuators for the spinning vehicle need to synchronize with the spin frequency and phase in order to make a turn or pitch.

To accurately control the flight path of the spinning vehicle, the control system needs to eliminate the interference caused by the spin. Usually the actuators (either canards or thrusts) are located symmetrically around the cylinder for the control of yaw and pitch of the vehicle. For instance, four canards are placed 90 degree apart from each other on a surface circle around the spinning axis. When in operation, the four canards will oscillate at the same frequency as the vehicle spinning frequency and with 90 degree phase shift from one another.

Now, it is clear that the canards need to oscillate following a sinusoidal tracking signal. The frequency of the tracking signal is the same as that of the spinning vehicle, the amplitude is determined by the magnitude of the desired flight-path change and the phase is by both the vehicle spinning phase and the direction of desired flight-path change.

Therefore, the problem can be formulated as a sinusoidal tracking control problem, in which the canards are controlled to follow the sinusoidal tracking signals as closely as possible. The tracking/regulator control problem has been intensively studied in the literature [1-8], especially the asymptotic tracking/regulation in the continuous-time case. In addition to the internal model principle [1-6] that guarantees zero steady-state tracking error, in this paper, the optimal H_2 / H_∞ control theory [9-11] is employed to optimize the transient response and the robustness subject to control input constraints.

Since the controller will be implemented in a DSP microprocessor (Texas Instruments TMS320F2812), it will be designed in discrete time. The canards are driven by a DC motor, whose input DC voltage and therefore the output angular position are dictated by the output of the controller. A digital-to-analog conversion (DAC) unit needs to serve as the interface between the digital controller and the analog DC motor. Due to less power consumption and size advantage over the traditional zero-order-hold (z.o.h.) type DAC, the PWM (pulse waveform modulation) channels inside the DSP microprocessor chip appears a better alternative and will be used in the hardware implementation. Nevertheless, the zero-order-hold [12-14] is still employed to characterize the DAC unit in the design process because of the following two reasons: 1) the PWM in many cases is a good approximation of the zero-order-hold [15], and 2) a PWM control system design theory is still not available [15,16]. An optical encoder together with the timers and counters in the DSP microprocessor is used to measure the angular displacement and velocity of the motor.

The rest of the paper is organized as follows. In section II, the canard control under the influence of persistent spin is formulated as a sinusoidal tracking problem. In section III, a discrete-time controller design procedure is given to not only provide steady-state tracking, fast transient response but also address the robustness and the control-input-

** Research supported in part by Army Research Laboratory under contract DAAD17-03-P-0422 and in part by NASA under contract NAG-1-01118.
* Corresponding Author, Phone: 215-895-1790, Fax:215-895-1478, e-mail: bchang@coe.drexel.edu

constraint issues. Numerical time-domain simulations are performed in section IV for the closed-loop sampled-data system with z.o.h. and with PWM. In section V, the same optimal tracking controller is implemented on the Texas Instruments DSP microprocessor TMS320F2812, which shows that the real-time tracking performance is very close to the simulation results. Concluding remarks are given in section VI.

II. PROBLEM FORMULATION AND STEADY-STATE TRACKING

The spinning flying vehicle is equipped with four canards uniformly allocated around the cone-shaped front end of the vehicle. They would coordinate and oscillate according to the spin to make a turn or a pitch. The tracking signal for one of the canards will be of the form, $A_r \sin(\omega t + \varphi)$, where ω is the same as the spinning frequency of the vehicle, A_r, the deflection of canard, reflects the magnitude of the flight-path change, and φ is determined by both the phase of the spinning vehicle and the direction of flight-path change. The desired angular positions for the next three canards will be of the same frequency, same magnitude, but with 90 degree phase lag. A mechanical coupling (bevel gear) can be used to link the four canards so that they oscillate at the same frequency, the same amplitude, but with 90 degree phase lag one after another.

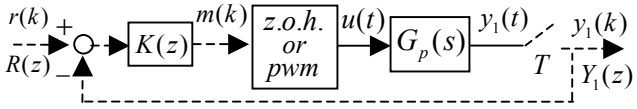

(a) typical sampled-data control system

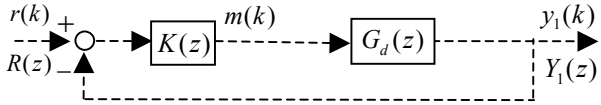

(b) discrete-time equivalent of (a) with z.o.h.

Fig. 2.1 Sampled-data feedback control system.

In the control system block diagram as shown in Fig.2.1(a), $G_p(s)$ is the analog plant to be controlled, which in our case is the DC motor together with the canard assembly. The zero order hold *z.o.h.* converts the discrete-time signal $m(k)$ into a continuous-time $u(t)$. On the other hand, the sampler T converts the continuous-time signal $y_1(t)$ into a discrete-time sequence $y_1(k)$, which actually is $y_1(kT)$. The objective is to find a discrete-time controller $K(z)$ so that the closed-loop system is stable and the output $y_1(k)$ follows the reference input $r(k) = A_r \sin(\omega kT + \varphi)$ as closely as possible. Note that in these block diagrams, the dotted lines represent discrete-time signals and the solid lines are for the continuous-time signals. The *z.o.h.* eventually will be replaced by PWM in implementation for practical reasons.

The combination of the zero order hold, *z.o.h.*, the analog plant, $G_p(s)$, and the sampler T can be represented by a discrete-time system $G_d(z)$ [12-14] and hence Fig.2.1(a) has its discrete-time equivalent as shown in Fig.2.1(b). It is well known that the Bode plots of the closed-loop transfer function $G_f(z) = G_d(z)K(z)/(1 + G_d(z)K(z))$ contain useful frequency-domain information in determining sinusoidal steady-state response. Let

$$G_f(e^{j\omega T}) = \left|G_f(e^{j\omega T})\right| \angle G_f(e^{j\omega T})$$

Then the steady-state response of the closed-loop system to the reference input, $r(k) = A_r \sin(\omega kT + \varphi)$, will be

$$y_{1ss}(k) = \left|G_f(e^{j\omega T})\right| A_r \sin(\omega kT + \varphi + \angle G_f(e^{j\omega T}))$$

If the controller $K(z)$ is chosen so that $\left|G_f(e^{j\omega T})\right| = 1$ and $\angle G_f(e^{j\omega T}) = 0^\circ$, then the steady-state output will be identical to the reference input. This asymptotic tracking (with zero steady-state tracking error) can be achieved by incorporating the internal model of the tracking signal into the loop transfer function of the closed-loop system.

III. DESIGN OF DISCRETE-TIME OPTIMAL SINUSOIDAL TRACKING CONTROLLER

In this section, a discrete-time state-space design approach will be given to achieve steady-state tracking, optimize the transient response, and address the robustness issues subject to the control-input constraints.

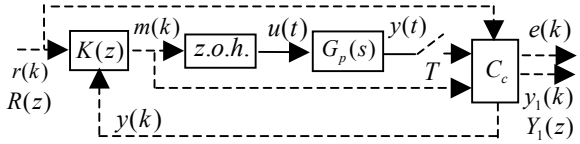

(a) sampled-data feedback control system

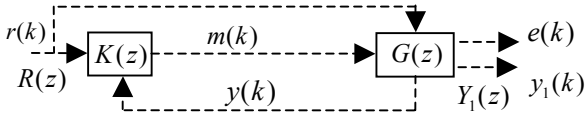

(b) discrete-time equivalent of (a)

Fig. 3.1 Sampled-data feedback control system and its discrete-time equivalent

The tracking command (reference input) can be described as the output of an exogenous system with the following state-space model:

$$\begin{aligned} \theta_R(k+1) &= Z_d \theta_R(k) + W_r w_r(k) \\ r(k) &= C_r \theta_R(k) + v_r(k) \end{aligned} \qquad (3\text{-}1a)$$

where w_r and v_r are white noises with the following covariance matrices:

$$E(w_r w_r^T) = Q_r,\ E(v_r v_r^T) = V_r,\ E(w_r v_r^T) = 0 \qquad (3\text{-}1b)$$

A more general sampled-data feedback control system block diagram is shown in Fig.3.1a. The state-space model of the analog plant is given as

$$G_p(s): \quad \dot{x}(t) = A_p x(t) + B_{p2} u(t) \qquad (3\text{-}2a)$$

$$y(t) = C_2 x(t) \qquad (3\text{-}2b)$$

where $y(t)$ is the measured output vector which includes all the measurable variable. The output variable $y_1(t)$, which is required to follow the reference input, is assumed part of the vector $y(t)$. Again, the solid lines in the block diagram represent continuous-time signals and the dotted lines are the sampled discrete-time signals. The box C_c represents a signal distributor that defines the controlled output vector

$$e(k) = \begin{bmatrix} e_1(k) \\ e_2(k) \end{bmatrix} = \begin{bmatrix} C_r \theta_R(k) - y_1(k) \\ D_{12d} m(k) \end{bmatrix} \tag{3-3}$$

in which $e_1(k)$ is the tracking error and $e_2(k)$ is the weighted control input.

Let $\Phi(t)$ be the state transition matrix for the analog plant,

$$\text{i.e.,} \qquad \Phi(t) = \sum_{k=0}^{\infty} (A_p t)^k / k! \tag{3-4}$$

Then the combination of the zero-order-hold, the analog plant, the sampler with sampling period T, and the signal distributor C_c can be replaced by the following discrete-time equivalent state-space model,

$$G(z): \quad x(k+1) = Ax(k) + B_1 w_1(k) + B_2 m(k) \tag{3-5a}$$

$$e(k) = \begin{bmatrix} C_{1u} \\ 0 \end{bmatrix} x(k) + \begin{bmatrix} D_{11u} \\ 0 \end{bmatrix} \theta_R(k) + \begin{bmatrix} 0 \\ D_{12d} \end{bmatrix} m(k) \tag{3-5b}$$

$$y(k) = C_2 x(k) + v(k) \tag{3-5c}$$

where $D_{11u} = C_r$ and

$$A = \Phi(T) \tag{3-6a}$$

$$B_2 = \left[\int_0^T \Phi(T-\lambda) d\lambda \right] B_{p2} \tag{3-6b}$$

and w_1 and v are assumed white noises with the following covariance matrices:

$$E(w_1 w_1^T) = Q_o, \quad E(vv^T) = R_o, \quad E(w_1 v^T) = N_o \tag{3-6c}$$

Let

$$\bar{x}(k) = x(k) - W\theta_R(k) \text{ and } \bar{m}(k) = m(k) - U\theta_R(k) \tag{3-7a}$$

where W and U are chosen such that

$$\begin{aligned} AW + B_2 U - WZ_d &= 0 \\ C_{1u} W + D_{11u} &= 0 \end{aligned} \tag{3-7b}$$

Then

$$\bar{x}(k+1) = A\bar{x}(k) + B_1 w_1(k) - WW_r w_r(k) + B_2 \bar{m}(k) \tag{3-8a}$$

and

$$e(k) = \begin{bmatrix} e_1(k) \\ e_2(k) \end{bmatrix} = \begin{bmatrix} C_{1u} \\ 0 \end{bmatrix} \bar{x}(k) + \begin{bmatrix} 0 \\ D_{12d} \end{bmatrix} \bar{m}(k) \tag{3-8b}$$

Now the problem is to find a discrete-time controller $K(z)$ so that

1) the closed-loop system is internally stable,

2) the tracking error is zero at steady state, and,

3) the following cost function is minimized

$$J = \lim_{N\to\infty} \frac{1}{N} E\left[\sum_{k=0}^{N} e^T(k) e(k) \right] \tag{3-9}$$

where $E[X]$ stands for the expectation of the stochastic signal X.

The designed discrete-time controller has the structure shown in Fig. 3.2, in which the U and W matrices guarantee steady-state tracking and the state feedback gain matrix F is chosen to tradeoff among the transient response, robustness, and control-input constraint.

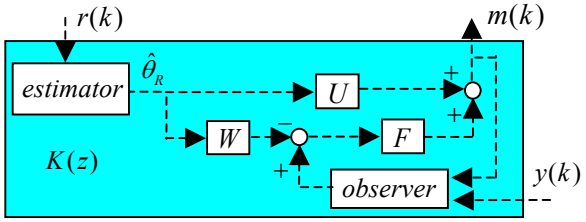

Fig. 3.2 Structure of the controller

Steady-state Regulation

According to the regulator theory [4-6], zero-steady-state-error tracking is achievable only if there exist constant matrices W and U so that the equations in (3-7b) are satisfied.

Estimator Construction

The estimator in Fig.3.2 is employed to estimate the states of the exogenous system of (3-1a). If (Z_d, C_r) is detectable, a stable estimator can be constructed as follows,

$$\hat{\theta}_R(k+1) = \left(Z_d - L_r C_r\right) \hat{\theta}_R(k) + L_r r(k) \tag{3-10a}$$

where the estimator gain L_r is

$$L_r = Z_d Y_r C_r^T (V_r + C_r Y_r C_r^T)^{-1} \tag{3-10b}$$

and Y_r is the positive semi-definite stabilizing solution of the following algebraic Riccati equation,

$$Z_d Y_r Z_d^T - Z_d Y_r C_r^T (V_r + C_r Y_r C_r^T)^{-1} C_r Y_r Z_d^T + W_r Q_r W_r^T = Y_r \tag{3.10c}$$

where Q_r and V_r are covariance matrices defined in Equation (3-1b).

State Feedback Gain F

Define

$$Q = C_{1u}^T W_Q^T W_Q C_{1u}, \qquad R = D_{12d}^T W_R^T W_R D_{12d} \tag{3-11a}$$

Then the state feedback gain matrix F can be computed as follows,

$$F = -(B_2^T X B_2 + R)^{-1} B_2^T X A \tag{3-11b}$$

where X is the positive semi-definite stabilizing solution of the following algebraic Riccati equation,

$$A^T XA - A^T XB_2(R + B_2^T XB_2)^{-1} B_2^T XA + Q = X \quad \text{(3-11c)}$$

Construction of Observer

If (A, C_2) is detectable, a stable observer can be constructed as follows,

$$\hat{x}(k+1) = (A - LC_2)x(k) + B_2 m(k) + Ly(k) \quad \text{(3-12a)}$$

where the observer gain L is

$$L = AY_o C_2^T (R_o + C_2 Y_o C_2^T)^{-1} \quad \text{(3-12b)}$$

and Y_o is the positive semi-definite stabilizing solution of the following algebraic Riccati equation,

$$AY_o A^T - (AY_o C_2^T + N_o)(R_o + C_2 Y_o C_2^T)^{-1}(C_2 Y_o A^T + N_o^T) + Q_o = Y_o \quad \text{(3-12c)}$$

where Q_o, R_o, N_o are covariance matrices defined in Eq. (3-6c). If all the state variables are available, i.e., $y(k) = x(k)$, then the observer can be omitted.

IV. NUMERICAL RESULTS AND COMPUTER SIMULATION

The analog plant, the DC motor with canards, is assumed to be a second-order linear model with state equation shown in eq.(3-2a) with

$$A_p = \begin{bmatrix} 0 & 1 \\ 0 & -4.2 \end{bmatrix}, \quad B_p = \begin{bmatrix} 0 \\ 34 \end{bmatrix} \quad \text{(4-1)}$$

and $C_2 = I_2$, i.e., all the two state variables, angular position x_1 and angular velocity x_2, are available for feedback. Recall that the objective is to design a controller so that the tracked output y_1, which is the angular position x_1 in this example, follows the tracking input signal r as closely as possible. The discrete-time equivalent of the analog plant can be found using eq. (3-5a).

The tracking signal is assumed of the form

$$r(t) = A_r \sin(\omega t + \varphi) \text{ or } r(k) = A_r \sin(\omega kT + \varphi) \quad \text{(4-2)}$$

where the amplitude A_r and the phase φ are arbitrary and the frequency ω is between 5 rad/s and 20 rad/s. In the design, we will choose the sampling period $T = 1\,ms$ and ω =10 rad/s. Then the exogenous system for the tracking signal can be represented by eq. (3-1a).

The controlled output $e(k)$ is defined by eqs. (3-3) or (3-5b) with

$$C_{1u} = \begin{bmatrix} -1 & 0 \end{bmatrix}, \quad D_{11u} = \begin{bmatrix} 1 & 0 \end{bmatrix}, \quad D_{12d} = 0.1 \quad \text{(4-3)}$$

The steady-state regulation matrices W and U can be found from Eq. (3-7b). Using Eq. (3-10a), we have the exogenous system estimator constructed with the estimator gain L_r, which is obtained according to Eqs.(3-10b) and (3-10c) based on $Q_r = 10^6 I_2, V_r = 10^{-6}$. In determining the state feedback gain F, we choose the weighting matrices Q and R as shown in Eq. (3-11a) with C_{1u} and D_{11u} given by Eq. (4-4) and $W_Q = 10$ and $W_R = 0.1$. Then from Eqs. (3-11b) and 3-11c) we have the state feedback gain F.

Now, we have the controller as shown in Fig.4.1. With this controller, draw the Bode plots for the closed-loop system transfer function from the tracking input $R(z)$ to the tracked output $Y_1(z)$, you will see that the magnitude response is 0 dB and the phase is 0° at 10 rad/s, which means the system has perfect steady-state tracking at 10 rad/s. In addition, the Bode plots are pretty flat for the frequency range between 5 rad/s and 20 rad/s.

The simulation diagram shown in Fig.4.1 will be used to conduct sinusoidal tracking simulations to check if all design specifications are met. Recall that $x_1(t)$, the angular displacement of the DC motor, is required to closely follow the tracking input $r(t)$, a sinusoidal signal with the frequency ranging from 5 rad/s to 20 rad/s and arbitrary amplitude and phase. The control input $u(t)$ is limited to ± 12 volts. In practice, either *z.o.h.* or PWM can be used to implement the digital to analog conversion (ADC). The PWM consumes less power that results in smaller, lighter, and less expensive hardware implementation. Since there is no available control systems design theory developed based on PWM as the ADC, the common practice is to employ the existing digital control theory, which has been well developed based on *z.o.h.* as the ADC, to design a controller and then replace the *z.o.h.* by PWM in the real time implementation. Usually it is a good approximation if the frequency of the PWM waveform is high enough.

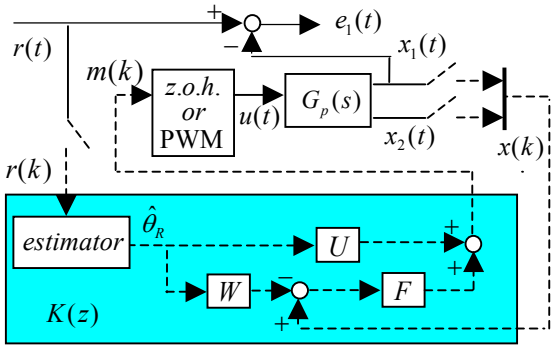

Fig.4.1 Closed-loop simulation diagram with the optimal discrete-time sinusoidal tracking controller

First of all, a simulation will be conducted for the tracking signal $r(t) = 0.5 \sin 10t$ with *z.o.h.* as the ADC. The $0.5\,rad$ amplitude means that the desired output would oscillate between $\pm 28.65^\circ$.

With the controller designed above, the tracking response virtually coincides with the tracking command. However, the control effort in the beginning reaches 45V, which is beyond the 12V limit. It will be seen that this over design provides better performance because of the more effective

use of the control input. The simulation results with a 12V Saturator are shown in Fig.4.2. The performance is almost perfect except for the short period of time in the very beginning.

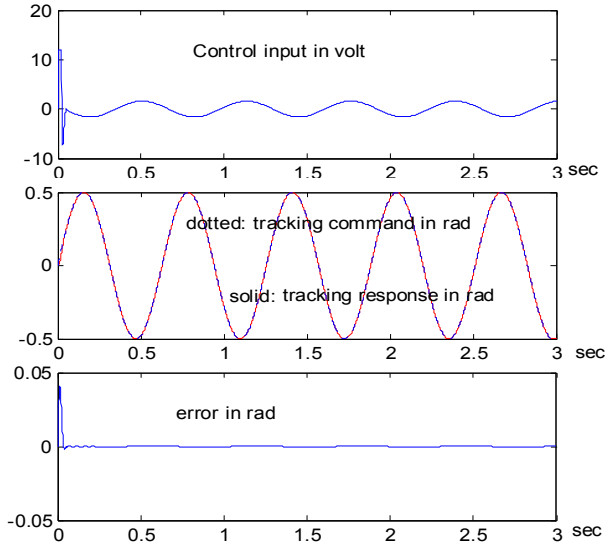

Fig.4.2 Simulation result for $r(t) = 0.5\sin 10t$ with z.o.h. and 12V control input limit

Now, the simulation results with the *z.o.h.* replaced by PWM are shown in Fig.4.3. The performance deteriorates a little bit; however, the maximum steady state error is still less than 0.5 %.

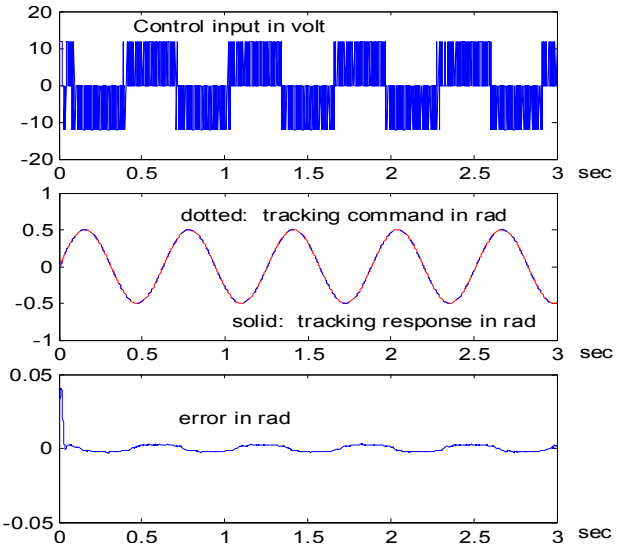

Fig.4.3 Simulation result for $r(t) = 0.5\sin 10t$ with PWM

Recall that the controller was designed to track a sinusoid with frequency at 10 rad/s. To see if the same controller works well for the tracking signals at 5rad/s and 20rad/s, simulations are conducted for $r(t) = 0.5\sin 5t$ and $r(t) = 0.5\sin 20t$ with PWM serving as the ADC. The steady-state tracking error for 5 rad/s signal is about 0.4% and for 20 rad/s signal is less than 2.4%.

V. DSP MICROPROCESSOR IMPLEMENTATION OF THE SINUSOIDAL TRACKING CONTROLLER

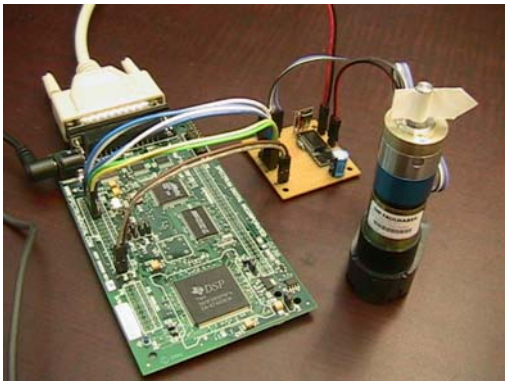

Fig.5.1 Experimental setup for real time sinusoidal tracking

The same controller used in the previous section for simulations will be implemented in a DSP microprocessor to drive a DC motor for sinusoidal tracking. As shown in Fig.5.1, the experimental setup includes a Faulhaber DC-Micro-motor 2230 with optical encoder HEDS5540, a Texas Instruments H-bridge circuit TPIC0108C, and a Texas Instruments DSP microprocessor TMS320F2812 eZ-DSP board.

The 150MHz, 32-bit with 64-bit processing capability DSP microprocessor has built-in ADC, QEP (quadrature-encoder pulse circuit) and PWM[17]. The QEP is used together with the optical encoder to measure the angular displacement and velocity of the motor. The PWM is employed to achieve digital-to-analog conversion and the frequency of the PWM waveform is chosen to be 2.2 *kHz* and the amplitude is 12*V*. The sampling period for the controller implementation is 1 *ms*.

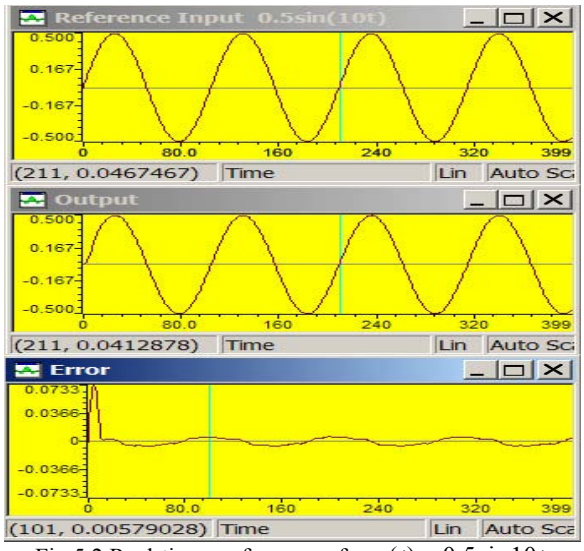

Fig.5.2 Real-time performance for $r(t) = 0.5\sin 10t$

Fig.5.2 shows the experimental results for the tracking command $r(t) = 0.5\sin 10t$. The vertical axis is the angular displacement in rad (57.3°) and horizontal axis is the time in 6 *ms*, for instance, the 320 mark actually means

1.92 *sec*. It can be seen that the reference input and the output are almost identical in both magnitude and phase. The steady-state error is less than 1.2%.

It is also desired that the steady-state tracking response is immune to the variation of frequency in the 5-20 rad/s. The same experiment was also conducted for the tracking inputs with frequencies at 5 rad/sec and 20 rad/sec. The steady-state tracking error is less than 1% for $r(t) = 0.5\sin 5t$. The tracking response starts to get worse when frequency increases to 20 rad/s. The maximum transient error is 53% and it takes 0.38 seconds to reach the steady state where the maximum tracking error is 9%.

The discrepancy between the computer simulation and the real-time results in the high frequency range comes from the fact that the plant model used in simulation is a simplified linear second-order system and the real DC motor is nonlinear with unmodeled dynamics. The high frequency switching PWM may also have aggravated the effect of the nonlinearity and unmodeled dynamics. A more realistic nonlinear plant model and a nonlinear controller design approach will certainly help. Furthermore, a frequency-weighted H_∞ control theory may be used to ensure a wider frequency band with 0dB magnitude and 0 degree phase for the closed-loop transfer function.

VI. CONCLUSION

In this paper, it is shown that the canard control of a spinning flying vehicle can be formulated as a sinusoidal tracking problem. An optimal regulator control theory was used to construct a controller that achieves stability, asymptotic tracking, minimal transient error, and robustness subject to control input constraints. The controller designed to track the 10 rad/s sinusoid is able to track all sinusoidal signals in the range of 1-20 rad/s using either z.o.h. or PWM as the DAC unit in simulation. The real-time implementation of the controller in the DSP microprocessor with PWM performs almost perfect tracking for the intended frequency and lower frequencies. The discrepancy between the computer simulation and real-time experiment in higher frequencies reveals the need of further research in the issues of nonlinearities, unmodeled dynamics, PWM high frequency switching, and the weighted H_∞ control design for better robustness.

VII. REFERENCES

[1] B. A. Francis, "The linear multivariable regulator problem," *SIAM J. Control and Optimization*, vol. 15, pp. 486-505, 1977.

[2] Linfu Cheng and J. B. Pearson, "Synthesis of Linear Multivariable Regulators," *IEEE Trans. On Automatic Control*, vol. AC-26, pp. 194-202, 1981.

[3] O.R. Gonzalez and P.J. Antsaklis, "Internal Models in Regulation, Stabilization, and Tracking," *IEEE Trans. On Automatic Control*, vol. AC-26, pp. 1343-1348, 1989.

[4] H. G. Kwatny and K.C. Kalnitsky, "On alternative methodologies for the design of robust linear multivariable regulators, " *IEEE Transactions on Automatic Control*, vol. AC-23, pp. 930-933, 1978.

[5] H. G. Kwatny and K-K D. Young, "The variable structure servomechanism," *Systems and Control Letters*, vol. 1, pp. 184-191, 1981.

[6] B. C. Chang, G. Bajpai, H. G. Kwatny, "A Regulator Design to Address Actuator Failures," *Proceedings of the 40th IEEE Conference on Decision and Control*, Volume: 2, pp. 1454 -1459, Dec. 2001.

[7] A. Lindquist and V. A. Yakubovich , "Universal Regulators for Optimal Tracking in Discrete-Time Systems Affected by Harmonic Disturbances," *IEEE Trans. On Automatic Control*, vol. AC-44, pp. 1688-1704, 1999.

[8] D. E. Miller and E. J. Davison, "The Self-Tuning Robust Servomechnism Problem," *IEEE Trans. On Automatic Control*, vol. AC-34, pp. 511-523, 1989.

[9] H. Kwakernaak and R. Sivan, *Linear Optimal Control Systems*, John Wiley & Sons, Inc., 1972.

[10] J. Doyle, K. Glover, P. Khargonekar and B. Francis, "State-space solutions to standard H_2 and H_∞ optimal control problems," *IEEE Transactions on Automatic control,* Vol. 33, pp. 831-847, 1989.

[11] K. Zhou, J. Doyle, K. Glover, *Robust and Optimal Control*, Prentice Hall, 1996.

[12] C. L. Phillips and H.T. Nagle, *Digital Control System Analysis and Design*, 3rd Edition, Prentice Hall, 1995.

[13] G. F. Franklin, M. L. Workman, and J.D. Powell, *Digital Control of Dynamic Systems*, 3rd Edition, Addison-Wesley, 1997.

[14] T. Chen and B. Francis, *Optimal Sampled-Data Control Systems*, Springer-Verlag, 1996.

[15] H. Sira-Ramirez, "A Geometric Approach to Pulse-Width Modulated Control in Nonlinear Dynamical Systems," *IEEE Trans. On Automatic Control,* Vol. 34, 1989.

[16] T.A. Sakharuk, B. Lehman, A.M. Stankovic, and G. Tadmor, "Effects of Finite Switching Frequency and Delay on PWM Controlled Systems," *IEEE Trans. On Circuits and Systems—I: Fundamental Theory and Applications,* Vol. 47, pp. 555 – 567, 2000.

[17] Texas Instrumnents, *TMS320F28x DSP Event Manager Refeference Guide*, Literature Number: SPRU065B, Nov. 2003.